Supporting information

A high-performance current collector-free flexible in-plane micro-supercapacitor based on highly conductive reduced graphene oxide film

Mingmao Wu, Yingru Li, Bowen Yao, Ji Chen, Chun Li and Gaoquan Shi**

Department of Chemistry, Tsinghua University, Beijing 100084, China

* Correspondence should be addressed to: chunli@mail.tsinghua.edu.cn; gshi@tsinghua.edu.cn

Supplementary Table

Table S1. Comparison of the electrochemical performances of various MSCs.

Material	Electrolyte	Areal Capacitance (mF cm^{-2})	Ref
LEG	H_3PO_4/PVA	13.01 at 0.01 V s^{-1} 8.59 at 1 V s^{-1}	this work
		11.15 at 1 mA cm^{-2} 15.38 at 0.1 mA cm^{-2}	
Onion carbon	1 M Et_4NBF_4 in PC	1.7 at 1 V s^{-1}	S1
Onion carbon	Ionic liquid[a]	1.1 at 0.2 V s^{-1}	S2
rGO	Hydrated GO	0.51	S3
Carbon	1 M Et_4NBF_4 in PC	2.1 at 0.001 V s^{-1}	S4
Porous carbon	Ionogel[b]	0.6 at 0.01 V s^{-1}	S5
LSG[c]	H_2SO_4/PVA	2.32 at 16.8 mA cm^{-3}	S6
LIG[d]	1 M H_2SO_4	3.9 at 0.2 mA cm^{-2}	S7
B-LIG[e]	H_2SO_4/PVA	12.4 at 0.04 mA cm^{-2}	S8
LIG	H_2SO_4/PVA	8.0 at 0.03 mA cm^{-2}	S9
LIG	H_3PO_4/PVA	0.8 at 0.01 V s^{-1}	S10
MPG[f]	H_2SO_4/PVA	0.0807	S11
Graphene	H_2SO_4/PVA	0.116 at 0.01 V s^{-1}	S12
rGO	H_2SO_4/PVA	0.95 at 0.43 mA cm^{-2}	S13
rGO/CNT[g]	3 M KCl	6.1 at 0.01 V s^{-1}	S14
MG/MWNTs[h]	H_3PO_4/PVA	2.54 at 0.01 V s^{-1}	S15
VACNTs[i]	Ionogel[j]	0.43 at 0.1 V s^{-1}	S16
rGO microribbons	H_3PO_4/PVA	0.54 at 0.5 V s^{-1}	S17
EG/PH1000[k]	H_2SO_4/PVA	5.4 at 0.001 V s^{-1}	S18

[a]This ionic liquid is composed of N-methyl-N-propylpiperidiniumbis[fluorosulfony]imide ($PIP_{13}FSI$) and N-butyl-N-N-methylpyrrolidiniumbis[fluorosulfony]imide ($PYR_{14}FSI$) in 1:1 ratio.

[b]This ionogel is composed of 1-ethyl-3-methylimidazolium bis(trifluoromethylsulfonyl)imide (EMI TFSI) and Fumed silica nanopowder (FS) in a 1:0.03 mass ratio.

[c]LSG is laser scribed graphene.

[d]LIG is laser-induced graphene.

[e]B-LIG is boron-doped laser-induced graphene.

[f]MPG is reduced graphene film.

[g]CNT is carbon nanotube.

[h]MG/MWNTs is multilayer graphene/multi-walled carbon nanotubes.

[i]VACNTs is vertical aligned carbon nanotubes.

[j]This ionogel is composed of tetramethyl orthosilicate (TMOS), formic acid (FA)and EMI TFSI in a 1:6:6 molar ratio.

[k]EG/PH1000 is electrochemically exfoliating graphene/electrochemically active poly(3,4-ethylenedioxythiophene):poly(styrenesulfonate)
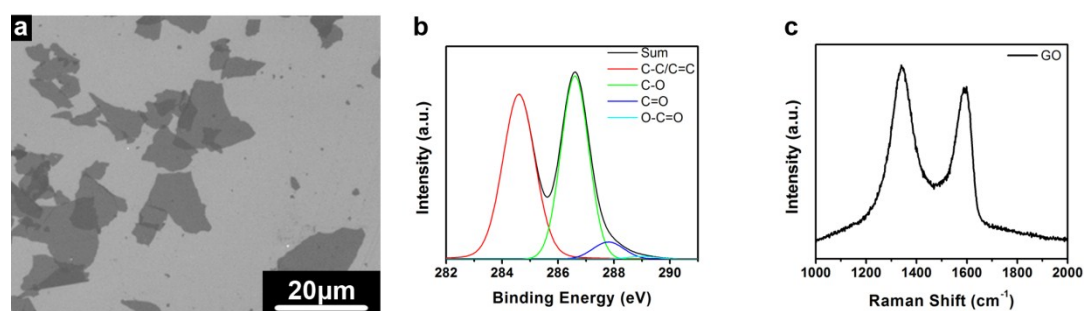
Supplementary Figures

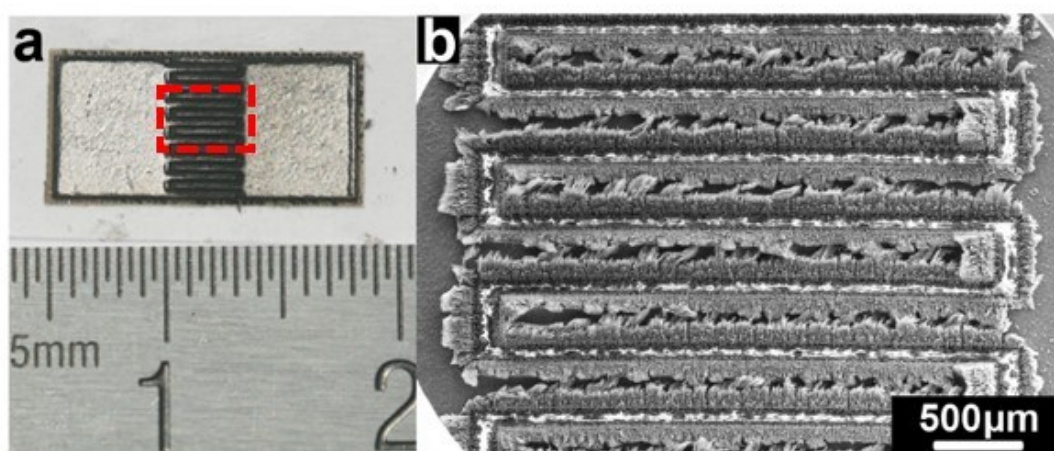**Fig. S1** (a) SEM image, (b) C 1s XPS spectrum and (c) Raman spectrum of GO sheets.

Fig. S2 (a) The photograph of a LG electrode composed of 8 pairs rGO fingers. (b) SEM image of the area circled by a red box in panel (a).
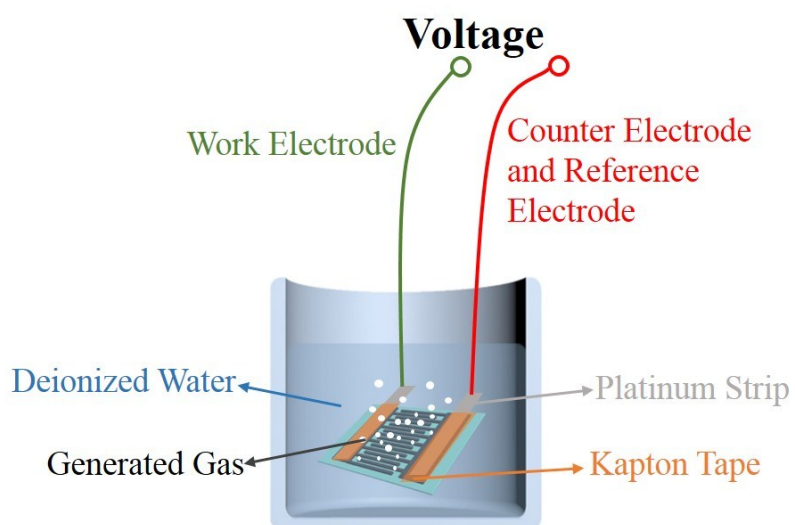

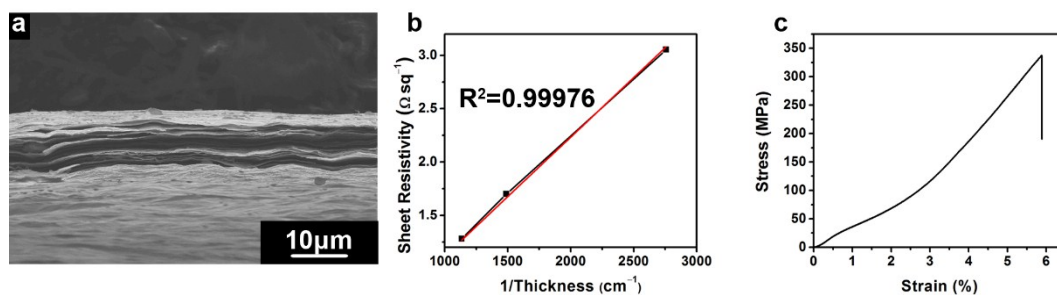**Fig. S3** Schematic illustration of the electrochemical activation process.

Fig. S4 (a) Cross section SEM image of an rGO/PVP composite film. (b) The relationship between the reciprocal of the thickness and sheet resistivity of rGO/PVP films. (c) Typical stress-strain curve of an rGO/PVP composite film.
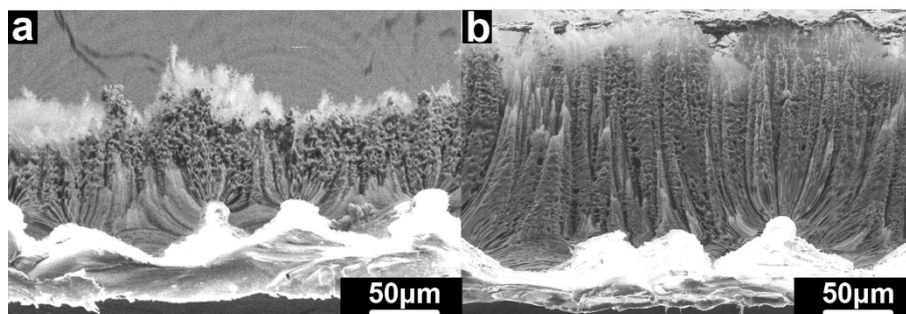

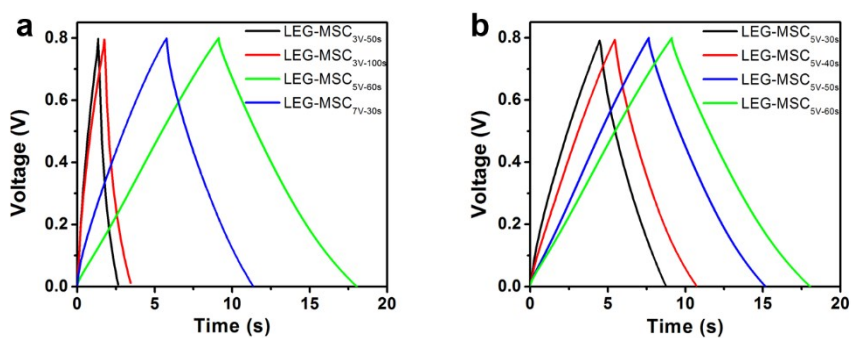**Fig. S5** Cross section SEM images of LG (a) and LEG (b) on PEN.

Fig. S6 The charge-discharge curves at 1 mA cm^{-2} for LEG-MSCs wih LEG-rGO electrodes treated by electrochemical activation (a) at 3 V for 50 or 100 s, or 5 V for 60 s or 7 V for 30 s or (b) at 5 V for 30, 40, 50 or 60 s; the voltages and time are dipicted in the names of MSCs (LEG-MSC$_{xV-ts}$, where x is the applied voltage, t is the given time in one direction).

Electrochemical activation of LG-rGO in water was applied to expand the compact rGO films. In this case, LG-rGO was subjected to a constant voltage (3, 5, or 7 V) for a given time (30, 40, 50, 60, or 100 s) and then at the opposite voltage for the same time. The resultant MSC is called LEG-MSC$_{xV\text{-}ts}$, where x is the applied voltage, t is the given time in one direction. It is expected that the rapid gas evolution by water electrolysis can expand the highly stacked rGO films into three-dimensional interconnected network. Indeed, it was found that 5 V and 60 s are the optimal combination of voltage and polarization time that can moderately expand the rGO film into porous network without detaching from the substrate. The MSC based on the LG treated at 5 V with 60 s followed by the opposite voltage with the same time gives a high areal capacitance of 11.15 mF cm^{-2} at the current density of 1.0 mA cm^{-2} (Fig. S6). Low voltage (3V) and short time ($\leq$ 50 s) are less efficient for the expansion of the rGO films due to the slow gas evolution rate and insufficient amount of gas produced, whereas high applied voltage (7 V) or long-time treatments usually detach the microelectrodes easily from the substrate (Fig. S6).
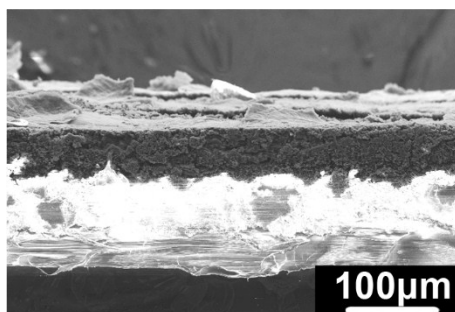

Fig. S7 Cross section SEM image of an LEG on PEN after pressing at 1 MPa for 1 min.
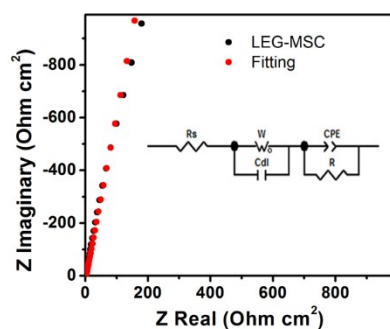
Fig. S8 Nyquist plot of the LEG-MSC (black circle) and fitting Nyquist plot of the device (red circle). The inset shows the equivalent circuit.

The inset of Fig. S8 shows the equivalent circuit of the device, where, R_S is the ohmic resistance attributed to the contact resistance between the interfaces of the electrolyte and electrodes, and the electrolyte resistance and electrode resistance. C_{dl} is the double layer capacitance. W is associated with the diffusion resistance of the porous electrode according to the DeLevie model. The parallel constant phase angle element (CPE) and R represent the leakage current from the oxygen function group reaction in low-frequency region.

Supplementary References

S1 D. Pech, M. Brunet, H. Durou, P. Huang, V. Mochalin, Y. Gogotsi, P. Taberna and P. Simon, *Nat. Nanotechnol.*, 2010, **5**, 651−654.

S2 P. Huang, D. Pech, R. Lin, J. K. McDonough, M. Brunet, P. L. Taberna, Y. Gogotsi and P. Simon, *Electrochem. Commun.*, 2013, **36**, 53−56.

S3 W. Gao, N. Singh, L. Song, Z. Liu, A. L. Reddy, L. Ci, R. Vajtai, Q. Zhang, B. Wei and P. M. Ajayan, *Nat. Nanotechnol.*, 2011, **6**, 496−500.

S4 D. Pech, M. Brunet, P. L. Taberna, P. Simon, N. Fabre, F. Mesnilgrente, V. Conédéra and H. Durou, *J. Power Sources*, 2010, **195**, 1266−1269.

S5 S. Wang, B. Hsia, C. Carraro and R. Maboudian, *J. Mater. Chem. A*, 2014, **2**,

7997−8002.

S6 M. F. El-Kady and R. B. Kaner, *Nat. Commun.*, 2013, **4**, 1475.

S7 J. Lin, Z. Peng, Y. Liu, F. Ruiz-Zepeda, R. Ye, E. L. Samuel, M. J. Yacaman, B. I. Yakobson and J. M. Tour, *Nat. Commun.*, 2014, **5**, 5714.

S8 Z. Peng, R. Ye, J. A. Mann, D. Zakhidov, Y. Li, P. R. Smalley, J. Lin and J. M. Tour, *ACS Nano*, 2015, **9**, 5868−5875.

S9 Z. Peng, J. Lin, R. Ye, E. L. Samuel and J. M. Tour, *ACS Appl. Mater. Interfaces*, 2015, **7**, 3414−3419.

S10 J. B. In, B. Hsia, J. H. Yoo, S. Hyun, C. Carraro, R. Maboudian and C. P. Grigoropoulos, *Carbon*, 2015, **83**, 144−151.

S11 Z.-S. Wu, K. Parvez, X. Feng and K. Müllen, *Nat. Commun.*, 2013, **4**, 2487.

S12 Z.-S. Wu, K. Parvez, X. Feng and K. Müllen, *J. Mater. Chem. A*, 2014, **2**, 8288−8293.

S13 Z.-K. Wu, Z. Lin, L. Li, B. Song, K. S. Moon, S. L. Bai and C.-P. Wong, *Nano Energy*, 2014, **10**, 222−228.

S14 M. Beidaghi and C. Wang, *Adv. Funct. Mater.*, 2012, **22**, 4501−4510.

S15 J. Yun, D. Kim, G. Lee and J. S. Ha, *Carbon*, 2014, **79**, 156−164.

S16 B. Hsia, J. Marschewski, S. Wang, J. B. In, C. Carraro, D. Poulikakos, C. P. Grigoropoulos and R. Maboudian, *Nanotechnology*, 2014, **25**, 055401.

S17 D. Qi, Z. Liu, Y. Liu, W. R. Leow, B. Zhu, H. Yang, J. Yu, W. Wang, H. Wang, S. Yin and X. Chen, *Adv. Mater.*, 2015, **27**, 5559−5566.

S18 Z. Liu, Z.-S. Wu, S. Yang, R. Dong, X. Feng and K. Müllen, *Adv. Mater.*, 2016, **28**, 2217−2222.